Supporting Information

High-performance ternary non-fullerene polymer solar cells with both improved photon harvesting and device stability

Manjun Xiao, Kai Zhang*, Sheng Dong, Qingwu Yin, Zixian Liu, Liqian Liu, Fei Huang*, and Yong Cao

Institute of Polymer Optoelectronic Materials and Devices, State Key Laboratory of Luminescent Materials and Devices, and State Key Laboratory of Pulp & Paper Engineering, and School of Materials Science and Engineering, South China University of Technology, Guangzhou 510640, China.

* Corresponding author.
E-mail address: mszhangk@scut.edu.cn (K. Zhang); msfhuang@scut.edu.cn (F. Huang).

Experimental Section

Fabrication and Characterization of Hole-only Devices

Devices were fabricated to measure electron and hole mobility by using the space-charge-limited current (SCLC) method. The device structure was ITO/PEDOT:PSS/BHJ/MoO_3/Ag and ITO/ZnO/BHJ/Ca/Al, respectively. The mobility was determined by fitting the dark current to the model of a single-carrier SCLC, which is described by the equation $J = (9/8)\varepsilon_0\varepsilon_r\mu((V^2)/(d^3))$, where J is the current, μ is the zero-field mobility, ε_0 is the permittivity of free space, ε_r is the relative permittivity of the material, d is the thickness of the active layers, and V is the effective voltage. The effective voltage was obtained by subtracting the built-in voltage (V_{bi}) and the voltage drop (V_s) from the series resistance of the whole device except for the active layers from the applied voltage (V_{appl}), $V = V_{appl} - V_{bi} - V_s$. The hole mobility can be calculated from the slope of the $J^{1/2}$~V curves.

Other Characterizations

UV-vis absorption spectra were recorded on a SHIMADZU UV-3600 spectrophotometer. Photoluminescence was measured with a SHIMADZU RF-5301PC fluorimeter. The EQE spectra measurements were performed on a commercial QE measurement system (QE-R3011, Enlitech). The transient photocurrent of the devices was measured by applying 530-nm laser pulses with a pulse width of 120 fs and a low pulse energy to the short-circuited devices in the dark. The laser pulses were generated from an optical parametric amplifier (TOPAS-Prime) pumped by a mode-locked Ti:sapphire oscillator-seeded regenerative amplifier with a pulse energy of 1.3 mJ at 800 nm and a repetition rate of 1 kHz (Spectra Physics Spitfire Ace). The photocurrent produced a transient voltage signal on a 50 Ω resistor, which was recorded by a Tektronix TDS3052C oscilloscope. Tapping-mode AFM images were obtained using a Nano Scope NS3A system (Digital Instruments, Inc.). TEM images were obtained using a JEM-2100F instrument.

Supporting Figures and Tables

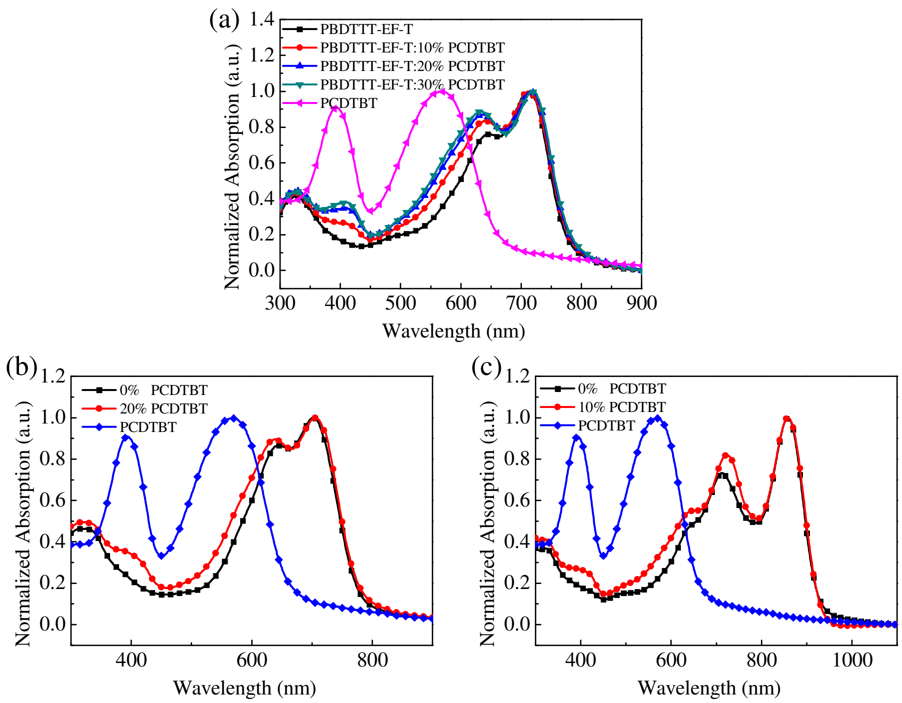

Figure S1. (a) The absorption spectra for PBDTTT-EF-T:PCDTBT films with different ratios. The normalized UV-vis absorption spectra of (b) PBDTTT-EF-T:ITIC, PBDTTT-EF-T:PCDTBT:ITIC, pure PCDTBT films and (c) PBDTTT-EF-T:IEICO-4F, PBDTTT-EF-T:PCDTBT:IEICO-4F, pure PCDTBT films.

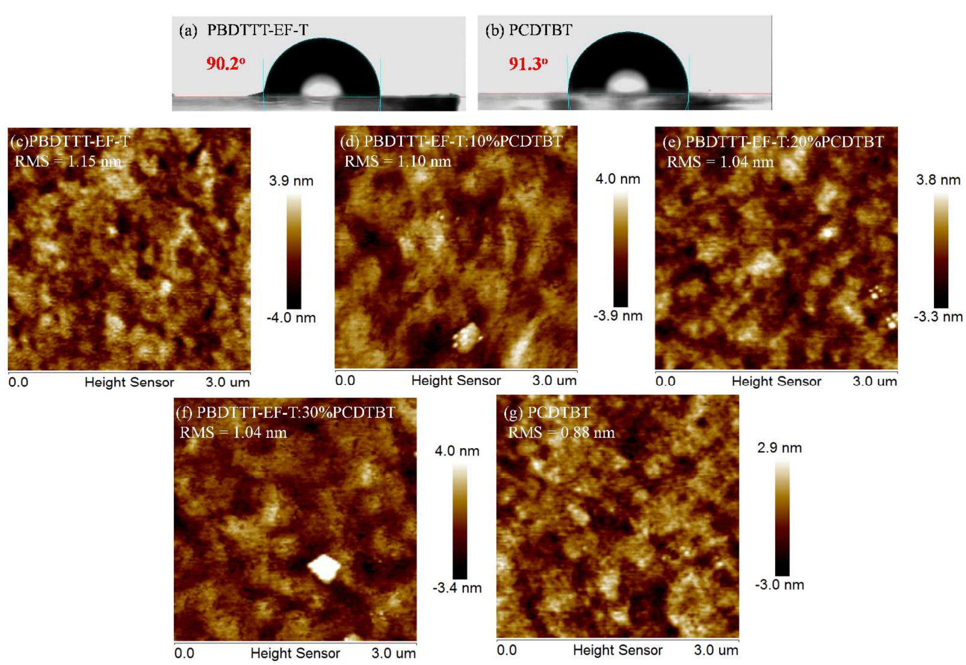

Figure S2. Contact angle measurements (DI water) of (a) PBDTTT-EF-T and (b) PCDTBT. The AFM images for (c) PBDTTT-EF-T pure film, (d) PBDTTT-EF-T:10%PCDTBT blend film, (e) PBDTTT-EF-T:20%PCDTBT blend film, (f) PBDTTT-EF-T:30%PCDTBT blend film and (g) PCDTBT film.

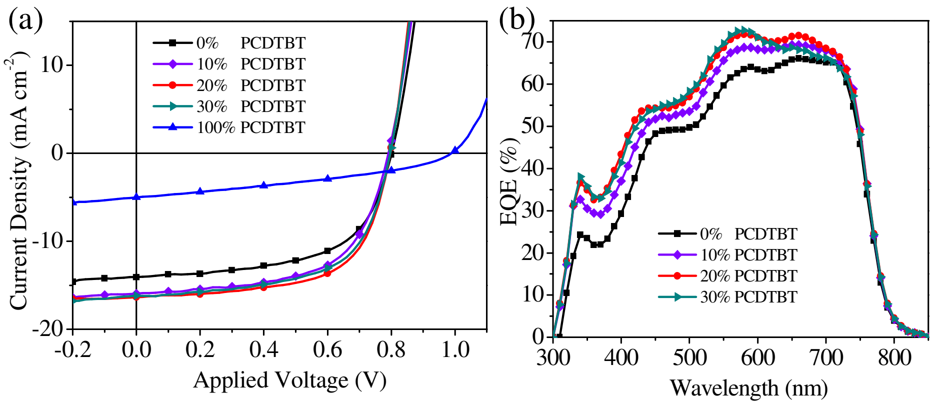

Figure S3. (a) $J-V$ curves and (b) EQE curves of binary and ternary system with a conventional device structure under AM1.5G illumination from a calibrated solar simulator under an irradiation intensity of 100 mW/cm^2.

Table S1. Summary of photovoltaic parameters of solar cells in a conventional device structure with different weight ratios of PCDTBT under AM1.5 illumination at 100 mW/cm^2

	PCDTBT Ratios	V_{oc} [V]	J_{sc} [mA cm^{-2}]	FF [%]	PCE [%]
	0%	0.80	14.09	59.10	6.67
	10%	0.79	15.95	60.47	7.63
PBDTTT-EF-T:x%PCDTBT :ITIC	20%	0.80	16.36	63.28	8.24
	30%	0.80	16.20	61.22	7.90
	100%	0.99	5.01	35.45	1.75

Table S2. Summary of photovoltaic parameters of PBDTTT-EF-T:PCDTBT:IEICO-4F-based polymer solar cells in a conventional device structure with different weight ratios of PCDTBT under AM1.5 illumination at 100 mW/cm^2

	PCDTBT Ratios	V_{oc} [V]	J_{sc} [mA cm^{-2}]	FF [%]	PCE [%]
	0%	0.72	22.19	66.36	10.63
PBDTTT-EF-T:x%PCDTBT:IEICO-4F	5%	0.72	23.14	68.18	11.33
	10%	0.72	24.03	70.36	12.15
	20%	0.71	23.27	68.39	11.25

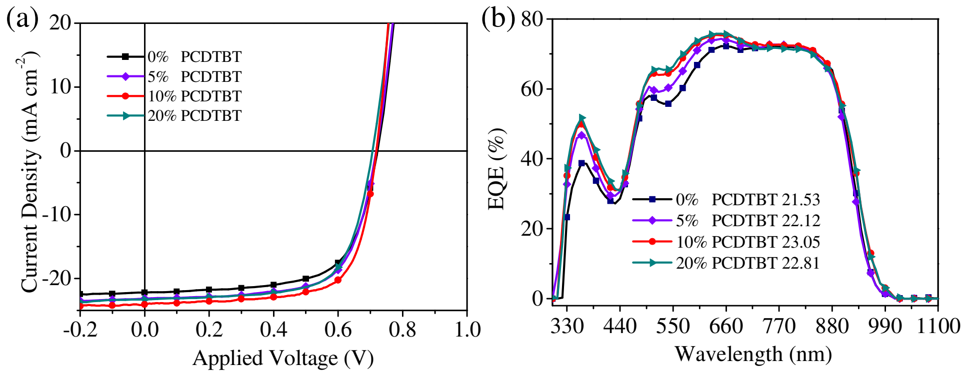

Figure S4. (a) $J-V$ curves and (b) EE curves of PBDTTT-EF-T:PCDTBT:IEICO-4F-based PSCs with a conventional device structure under AM1.5G illumination from a calibrated solar simulator under an irradiation intensity of 100 mW/cm^2.

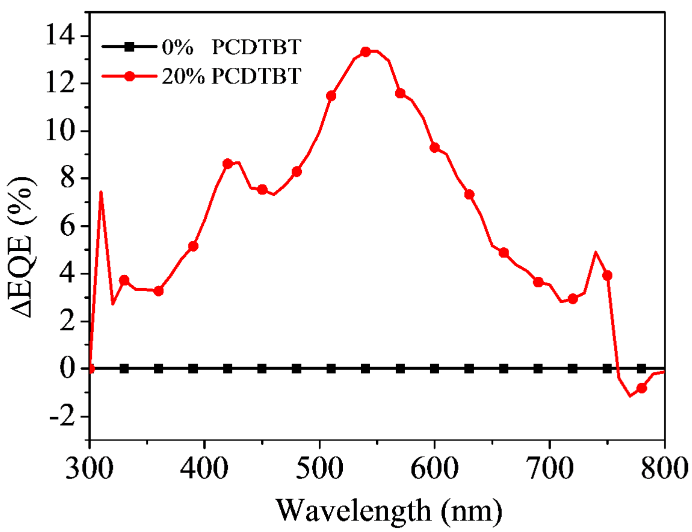

Figure S5. Δ EQE spectra between the optimized ternary PSCs and PBDTTT-EF-T-based binary PSCs.

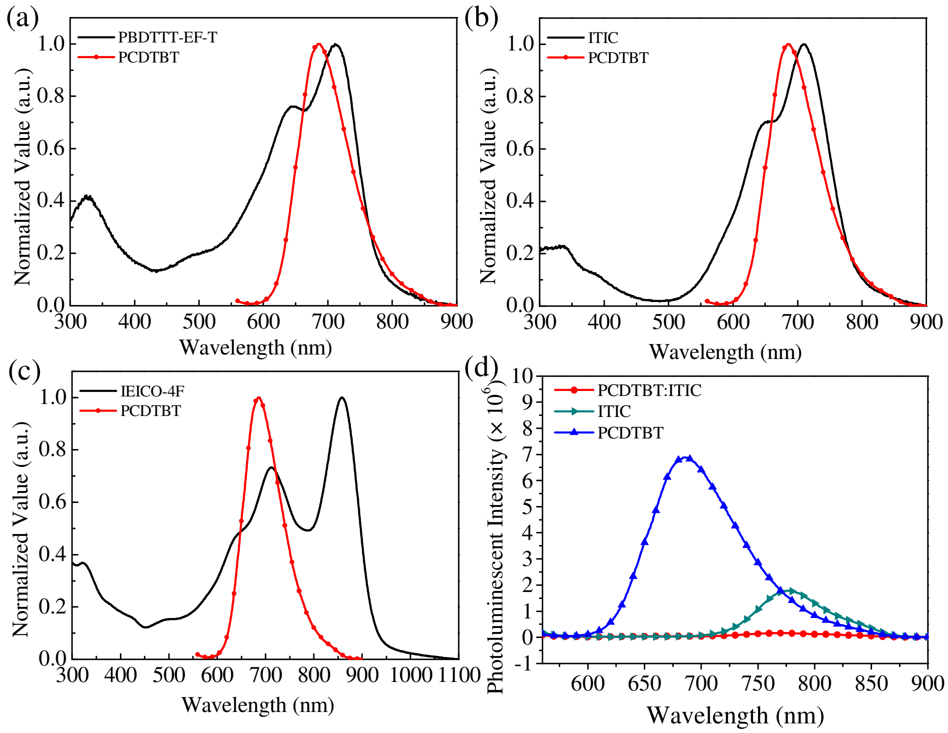

Figure S6. The Normalized absorption spectra of (a) PBDTTT-EF-T, (b) ITIC and (c) IEICO-4F with Photoluminescent spectrum of the pure PCDTBT films excited at 540 nm. (d) Photoluminescent spectra of the pure PCDTBT, ITIC and PCDTBT:ITIC binary films excited at 540 nm.

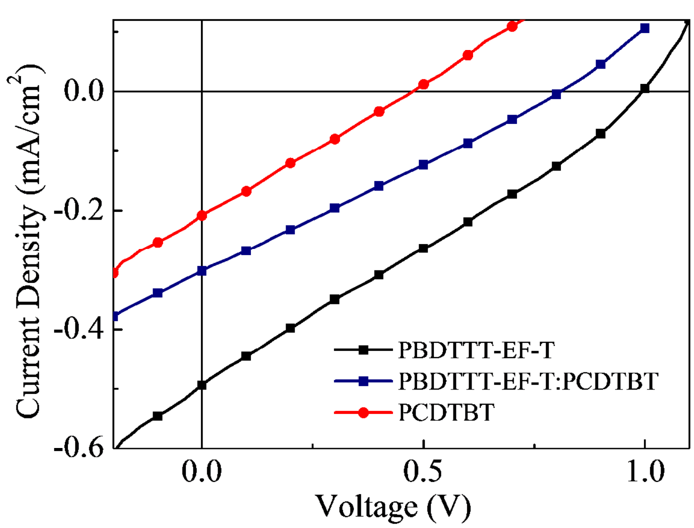

Figure S7. *J*−*V* curves of pure PBDTTT-EF-T-based device, pure PCDTBT-based device and PBDTTT-EF-T:PCDTBT-based binary device with a conventional device structure under AM1.5G illumination from a calibrated solar simulator under an irradiation intensity of 100 mW/cm^2.

Table S3. Summary of photovoltaic parameters of pure PBDTTT-EF-T-based device, pure PCDTBT-based device and PBDTTT-EF-T:PCDTBT-based binary device with a conventional device structure with different weight ratios of PCDTBT under AM1.5 illumination at 100 mW/cm^2.

PBDTTT-EF-T : PCDTBT	V_{oc} [V]	J_{sc} [mA cm^{-2}]	FF [%]	PCE [%]
1:0	0.99	0.49	27.26	0.13
1:1	0.81	0.30	26.06	0.06
0:1	0.48	0.21	25.31	0.03

Table S4. Relevant parameters obtained from J_{ph} - V_{eff} curves.

PCDTBT Ratios	V_0 [V]	J_{sat} [mA cm^{-2}]	G_{max} [m^{-3} s^{-1}]	$P(E,T)$ [a] [%]	$P(E,T)$ [b] [%]	L [nm]
0%	0.858	16.98	9.65×10^{27}	90.28	75.35	110
20%	0.865	18.71	1.11×10^{28}	94.94	77.97	105
100%	1.073	7.15	4.13×10^{27}	78.54	44.09	108

[a] under short-circuit condition.

[b] under maximal power output condition.

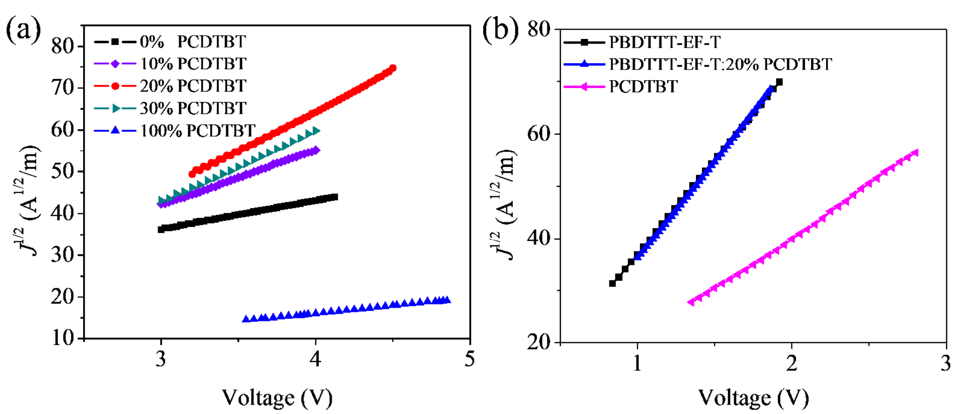

Figure S8. (a) Electron mobilities of the ternary devices with different weight ratios of PCDTBT in the ternary blends. (b) The hole mobilities for PBDTTT-EF-T:PCDTBT films with different ratios

Table S5. The calculated hole mobilities (μ_h) and electron mobilities (μ_e) of the ternary devices with different weight ratios of PCDTBT.

PCDTBT Ratio	μ_h [$cm^2 \cdot V^{-1} \cdot s^{-1}$]	μ_e [$cm^2 \cdot V^{-1} \cdot s^{-1}$]	μ_h/μ_e
0%	2.73×10^{-4}	3.05×10^{-5}	8.96
10%	2.90×10^{-4}	5.02×10^{-5}	5.78
20%	3.55×10^{-4}	9.45×10^{-5}	3.76
30%	3.29×10^{-4}	6.96×10^{-5}	4.73
100%	6.83×10^{-5}	3.33×10^{-6}	20.51

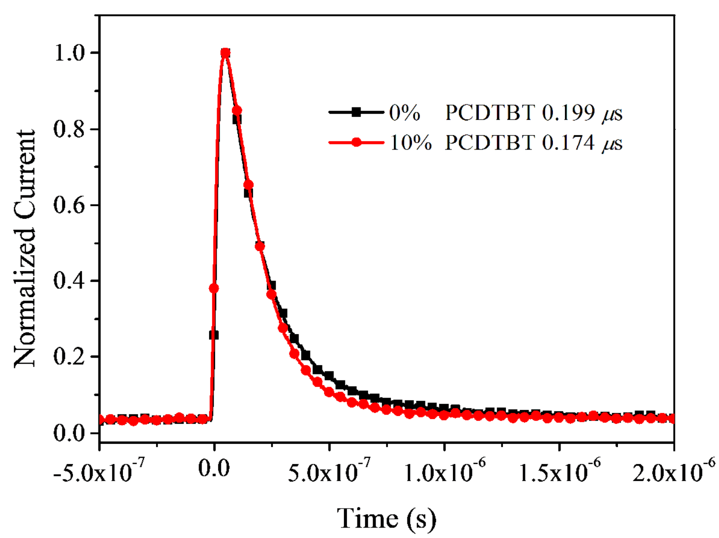

Figure S9. Transient photocurrent measurements of the IEICO-4F-based ternary devices with different weight ratios of PCDTBT in the ternary blends.

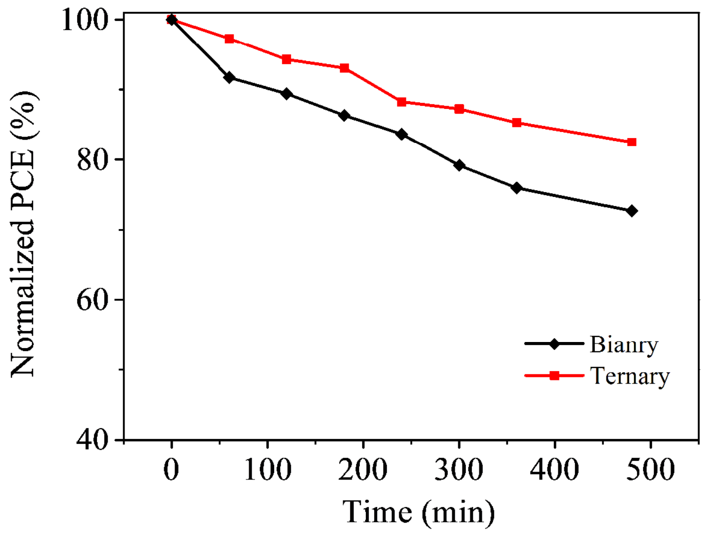

Figure S10. Stability of PSCs without encapsulation under AM 1.5G illumination at intensity of 100 mW cm^{-2}: the optimized binary and ternary PSCs with a conventional architecture were stored in air condition.

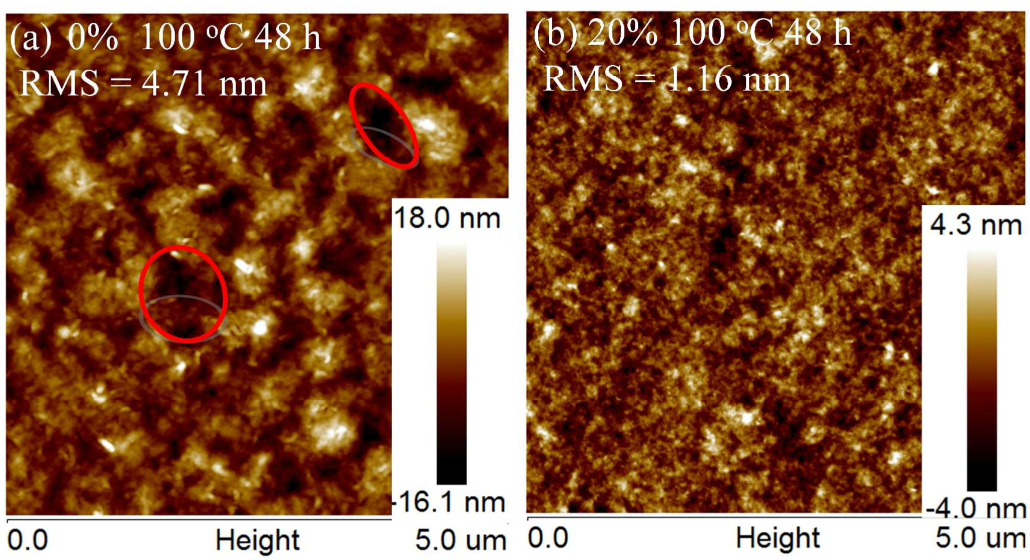

Figure S11. AFM images for PBDTTT-EF-T:ITIC blend films (a) without and (b) with PCDTBT content after 48 h thermal annealing at 100 ^{o}C.